



HAL
open science

Characterization of the Fireballs Detected by All-sky Cameras in Romania

Ioana Boaca, Maria Gritsevich, Mirel Birlan, Alin Nedelcu, Tudor Boaca, François Colas, Adrien Malgoyre, Brigitte Zanda, Pierre Vernazza

► **To cite this version:**

Ioana Boaca, Maria Gritsevich, Mirel Birlan, Alin Nedelcu, Tudor Boaca, et al.. Characterization of the Fireballs Detected by All-sky Cameras in Romania. *The Astrophysical Journal*, 2022, 936, 10.3847/1538-4357/ac8542 . insu-03780744

HAL Id: insu-03780744

<https://insu.hal.science/insu-03780744>

Submitted on 19 Sep 2022

HAL is a multi-disciplinary open access archive for the deposit and dissemination of scientific research documents, whether they are published or not. The documents may come from teaching and research institutions in France or abroad, or from public or private research centers.

L'archive ouverte pluridisciplinaire **HAL**, est destinée au dépôt et à la diffusion de documents scientifiques de niveau recherche, publiés ou non, émanant des établissements d'enseignement et de recherche français ou étrangers, des laboratoires publics ou privés.



Distributed under a Creative Commons Attribution 4.0 International License



Characterization of the Fireballs Detected by All-sky Cameras in Romania

Ioana Boaca¹ , Maria Gritsevich^{2,3} , Mirel Birlean^{1,4} , Alin Nedelcu^{1,4}, Tudor Boaca^{5,6} , François Colas⁴, Adrien Malgoyre⁷,
Brigitte Zanda⁴, and Pierre Vernazza⁸

¹ Astronomical Institute of the Romanian Academy, Str. Cutitul de Argint 5, 040557 Bucharest, Romania; ioana.boaca@astro.ro

² Finnish Geospatial Research Institute (FGI), Vuorimiehentie 5, FI-02150 Espoo, Finland

³ University of Helsinki, Faculty of Science, Gustaf Hällströmin katu 2, FI-00014 Helsinki, Finland

⁴ IMCCE, Observatoire de Paris, 77 av Denfert Rochereau, 75014 Paris Cedex, France

⁵ Department of Computer Science, Information Technology, Mathematics and Physics, Petroleum-Gas University of Ploiesti, 39 Bucharest Blvd Street, 100680 Ploiesti, Romania

⁶ Simion Stoilow Institute of Mathematics of the Romanian Academy, 21 Calea Grivitei Street, 010702 Bucharest, Romania

⁷ Service Informatique Pythéas (SIP) CNRS—OSU Institut Pythéas—UMS 3470, Marseille, France

⁸ Aix Marseille Univ, CNRS, CNES, LAM, Marseille, France

Received 2022 June 18; revised 2022 July 26; accepted 2022 July 27; published 2022 September 9

Abstract

Some of the fields of research that have captured the persistent interest of both scientists and the general public are meteor phenomena. The main goal in the study of meteoroid impacts into Earth's atmosphere is the recovery of the remnant matter after the ablation in the form of meteorites. This is a complementary approach, yet cheap alternative, to a sample return mission. Meteoroids are messengers since the time of the formation of the solar system due to the fact that they have preserved the same composition. The study of meteorites provides information regarding the chemical composition from which the planets formed. The increasing number of all-sky camera networks in recent years has resulted in a large set of events available for study. Thus, it is very important to use a method that determines whether the meteoroid could produce a meteorite or not. In this paper we study the meteors detected by the FRIPON network in Romania with the use of all-sky cameras. We focus on the events with noticeable deceleration ($V_f/V_0 < 0.8$). We determine the ballistic coefficient α and the mass-loss parameter β for the selected sample. Based on this analysis the events are classified in three categories: (1) meteoroids that are likely to produce meteorites; (2) meteoroids that can possibly produce meteorites; (3) meteoroids that are unlikely to produce meteorites. The entry and final mass are determined for each event. From the recorded fireballs, we identified one possible meteorite dropper, and we analyzed its dynamical evolution.

Unified Astronomy Thesaurus concepts: Meteoroids (1040); Meteors (1041); Meteorites (1038)

1. Introduction

Meteoroids are objects of asteroidal or cometary origin but smaller than asteroids, having diameters between 30 μm and 1 m. Meteoroids are produced by asteroid collisions, cometary activity, or disintegration, rotational disruption of low-strength asteroids (rubble-pile structure) via YORP, or during the close planetary approaches of asteroids by a tidal mechanism. Most of the objects entering the atmosphere vanish without hitting the ground. Given their origins and their production mechanism, the study of the population of meteoroids impacting the Earth's atmosphere is essential for understanding and evaluating the risk of space impacts.

The study of meteorites is of great importance because they have not modified their chemical composition since the formation of the solar system (Barucci et al. 2009). The recovery of meteoroid matter is very important because it provides scientific information comparable to a sample return mission. In order to systematically collect data about meteoroids entering the atmosphere and better characterize meteors and provide input for the current models of meteor physics, we developed a network of all-sky cameras over the Romanian territory called Meteorite Orbits Reconstruction by Optical Imaging (MOROI; Nedelcu et al. 2018) in 2017. In 2021 January the MOROI project was

integrated in The Fireball Recovery and Inter Planetary Observation Network (FRIPON). The meteors are detected with the use of a fish-eye lens with the focal length of 1.25 mm and the detector Sony ICX445. The data recorded by all FRIPON cameras are stored by the Service Informatique Pythéas (Aix-Marseille University, France; Colas et al. 2020). The coordinates of the FRIPON–MOROI cameras installed in Romania can be found in the Zenodo database (<https://doi.org/10.5281/zenodo.6626839>). The FRIPON project was started in 2016 by IMCCE, Observatoire de Paris. The purpose of the FRIPON project is to detect the meteors with the use of all-sky cameras, to determine their atmospheric trajectory, and compute the strewn field. At present, FRIPON contains more than 150 cameras and 25 European radio receivers over an area of $1.5 \times 10^6 \text{ km}^2$ (Colas et al. 2020). Cameras of FRIPON are installed in: Algeria, Australia, Austria, Belgium, Brazil, DOME—Canada, Chile, Denmark, Vigie-Ciel—France, Germany, PRISMA—Italia, Mexico, Morocco, Netherlands, MOROI—Romania, Peru, Senegal, South Africa, SPMN—Spain, Switzerland, Tunisia, SCAMP—UK (Colas et al. 2020). The detections of the FRIPON database can be found online.⁹ The meteoroids from the FRIPON database are denoted by the time when they were captured as year, month, day, followed by hour, minute, second in UT.

When a meteor is recorded by a camera observational network, we are able to determine its luminous 3D trajectory. If the meteoroid did not vanish during the ablation, fragments can

Original content from this work may be used under the terms of the [Creative Commons Attribution 4.0 licence](https://creativecommons.org/licenses/by/4.0/). Any further distribution of this work must maintain attribution to the author(s) and the title of the work, journal citation and DOI.

⁹ <https://fireball.fripon.org/>

remain and reach the ground in the form of meteorites. As will be shown in the following sections of this paper we are also able to identify those events producing meteorites from those not fully ablating in the atmosphere. The study of dark flight is essential in the process of the recovery of meteorites (Moilanen et al. 2021; Boaca et al. 2021).

Except for lunar rocks (Schmitt et al. 1970) and asteroid samples (Yoshikawa et al. 2015), the large variety of extraterrestrial material comes from meteorites. Lunar samples with a total weight of 300 kg were collected during the Apollo and Luna missions (Grady & Wright 2006). Among the most important collections of meteorites we mention: (i) National Meteorite Collection displayed at the Smithsonian National Museum of Natural History (Washington, D.C., United States) containing more than 55,000 samples from 20,000 different meteorites, (ii) the Meteorite Collection displayed at The Natural History Museum of Vienna¹⁰ containing 10,300 samples from 2550 different meteorites, (iii) The UCLA Meteorite Collection in the United States¹¹ with 2500 samples from about 1500 different meteorites.

In this paper we use a methodology of highlighting the most promising events out of the FRIPON database. In order to increase chances for meteorite recovery, following Sansom et al. (2019), we study the events with noticeable deceleration ($V_f/V_0 < 0.8$, where V_f is the velocity of the meteoroid at the end of the luminous trajectory and V_0 is the initial velocity of the meteoroid) detected by the FRIPON network after its installation in Romania. This allows us to narrow down the data set to a smaller sample with the most promising characteristics. The study is based on applying the α - β algorithm (Gritsevich 2008) to the FRIPON detections in order to determine the final outcome for the meteoroid, the initial mass, and the final mass of the meteoroid, respectively.

The structure of the paper is: Section 2 briefly presents the α - β algorithm, Section 3 describes the meteors detected by the FRIPON in Romania through the MOROI Network and the applications of the α - β algorithm, Section 4 presents the distribution of the α and β parameters for the selected fireballs (the application of the α - β algorithm to the MOROI detections with noticeable deceleration), while Section 5 presents the conclusion and perspectives for future work to be done.

2. The α - β Algorithm

The input parameters needed for our study are the meteor height and velocity. The algorithm used to identify a meteorite is the one proposed in Gritsevich (2008) and applied in Sansom et al. (2019). This algorithm is very useful and in our opinion this should be the first step a researcher should use in the study of meteoroids. Once the meteoroid height and velocity are determined, the final outcome (“likely fall,” “possible fall,” and “unlikely fall”) can be easily obtained (Sansom et al. 2019). This is of crucial importance when deciding which detected meteoroid can be chosen for the study of the dark-flight trajectory and for starting the campaign of searching the remnant matters on the ground.

Among other networks that have previously used this method we mention the Finnish Fireball Network (Lyytinen & Gritsevich 2016), the Desert Fireball Network (Sansom et al. 2019), the Spanish Meteor Network (Peña-Asensio et al. 2021a, 2021b), and the FRIPON (Drolshagen et al. 2021).

In this section we describe how to derive the parameters α and β from Gritsevich (2008) (Gritsevich et al. 2012). The starting point is given by the equations of motion of a meteoroid that are written under the following form (Gritsevich et al. 2017):

$$M \frac{dV}{dt} = -\frac{1}{2} c_d \rho_a V^2 S, \quad (1)$$

$$\frac{dh}{dt} = -V \sin \gamma, \quad (2)$$

$$H^* \frac{dM}{dt} = -\frac{1}{2} c_h \rho_a V^3 S. \quad (3)$$

The physical quantities that describe the motion in Equations (1)–(3) are: M is the mass of the meteoroid, V is the velocity of the meteoroid, γ is the slope of the trajectory, S is the cross-sectional area of the meteoroid, h is the height above the Earth’s surface of the meteoroid, ρ_a is the density of the atmosphere, H^* is the effective destruction enthalpy, c_h is the dimensionless heat transfer coefficient, and c_d is the drag coefficient.

In Gritsevich (2007) the Equations (1)–(3) are transformed in order to contain only dimensionless quantities. For this purpose the following transformations are made:

$$m = M/M_e, \quad (4)$$

$$v = V/V_e, \quad (5)$$

$$y = h/h_0, \quad (6)$$

$$s = S/S_e, \quad (7)$$

$$\rho = \rho_a/\rho_0, \quad (8)$$

where M_e is the mass of the meteoroid prior to the entry in the atmosphere, V_e is the velocity of the meteoroid at the entry in the atmosphere, h_0 represents the height of the homogeneous atmosphere, S_e is the cross-sectional area of the meteoroid at the moment of entry in the atmosphere, and ρ_0 is the density of air near the surface of the Earth.

The following equations are obtained using Equations (4)–(8) (Gritsevich 2007):

$$m \frac{dv}{dy} = \frac{1}{2} c_d \frac{\rho_0 h_0 S_e}{M_e} \frac{\rho v s}{\sin \gamma}, \quad (9)$$

$$\frac{dm}{dy} = \frac{1}{2} c_h \frac{\rho_0 h_0 S_e}{M_e} \frac{V_e^2}{H^*} \frac{\rho v^2 s}{\sin \gamma}. \quad (10)$$

The authors work under the hypothesis $s = m^\mu$ and consider the isothermal atmosphere: $\rho = \exp(-y)$. These conditions assure that Equations (9) and (10) have an analytical solution (Gritsevich 2008). Equations (9) and (10) have four unknown variables: m , v , s , and ρ . Thus the assumptions $s = m^\mu$ and $\rho = \exp(-y)$ allow us to solve Equations (9) and (10) (Gritsevich & Koschny 2011). The condition $s = m^\mu$ provides the association between the cross-sectional area of the meteoroid and its mass. The dimensionless parameter $\mu \in [0, 2/3]$ provides information related to the rotation of the meteoroid. Thus, if $\mu = 0$ then the meteoroid does not rotate at all. On the other hand, if $\mu = 2/3$ then the meteoroid rotates uniformly (Gritsevich 2008). As further seen in Section 4 of this work, the extreme values of $\mu = 0$ and $\mu = 2/3$ are used to classify the final outcome of the meteoroid, predicting whether a meteoroid is “likely,” “possibly,” or “unlikely” to produce meteorites.

¹⁰ <https://www.nhm-wien.ac.at>

¹¹ <https://meteorites.ucla.edu/>

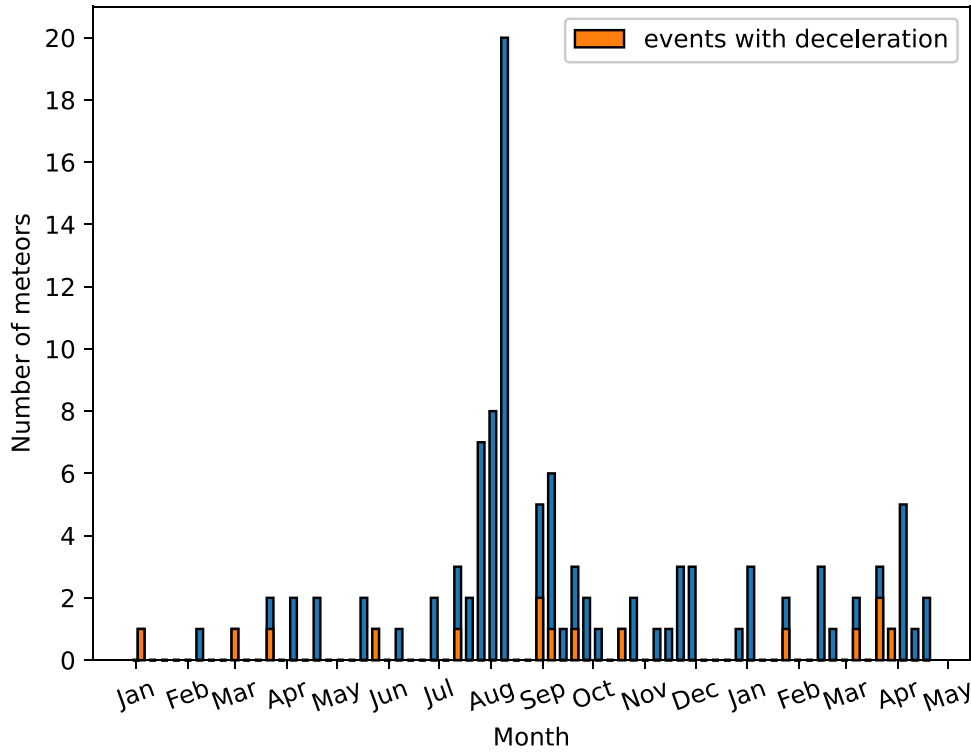


Figure 1. Number of weekly detections made by FRIPON in Romania during 2021–2022. The high number of meteors in August is due to the Perseid meteor shower.

The α – β algorithm has the possibility to be used with the arbitrary atmospheric model (Lyytinen & Gritsevich 2016). In Lyytinen & Gritsevich (2016) the authors study three fireballs recorded by the Finnish Fireball Network and determine the α and β parameters in the case of three types of atmospheres: the exponential atmosphere, the US Standard atmosphere (AIAA 2010), and the actual atmosphere. In Lyytinen & Gritsevich (2016) the actual atmosphere is derived using data from the Global Forecast System¹² and from the European Centre for Medium-Range Weather Forecast (ECMWF).¹³

With the boundary conditions: $y = \infty$, $v = 1$, $m = 1$ Equations (9) and (10) have the solutions (Gritsevich 2007):

$$m(v) = \exp\left(-\beta \frac{1 - v^2}{1 - \mu}\right), \quad (11)$$

$$y(v) = \ln 2\alpha + \beta - \ln(\bar{E}i(\beta) - \bar{E}i(\beta v^2)), \quad (12)$$

where

$$\bar{E}i(x) = \int_{-\infty}^x \frac{e^z dz}{z}$$

is the exponential-integral function (Abramowitz & Stegun 1964) and

$$\alpha = \frac{c_d \rho_0 h_0 S_e}{2M_e \sin \gamma}, \quad (13)$$

$$\beta = \frac{(1 - \mu) c_h V_e^2}{2c_d H^*}. \quad (14)$$

In (13) and (14) α is the ballistic coefficient and β is the mass-loss parameter.

The α and β parameters are the ones that minimize the expression (Gritsevich 2008):

$$Q_4(\alpha, \beta) = \sum_{i=1}^n (2\alpha \exp(-y_i) - \Delta_i \exp(-\beta))^2, \quad (15)$$

where

$$\Delta_i = \bar{E}i(\beta) - \bar{E}i(\beta v_i^2).$$

3. Results

In this section we present the applications of the algorithm described above to the FRIPON detections in Romania. These include the distribution of the α and β parameters, the final outcome of the meteoroid, and we compute the mass at the beginning and at the end of the luminous trajectory.

3.1. FRIPON Study Sample

In 2021 the Romanian all-sky cameras network (Nedelcu et al. 2018) was integrated in FRIPON (Jeanne et al. 2019; Colas et al. 2020). For our study we selected the detections that present noticeable deceleration ($V_f/V_0 < 0.8$) and that are well suited to be studied with the α – β algorithm presented in Section 2. The time period analyzed in our study is between 2021 January and 2022 April. In this period of time, 15 events that represent 13.88% of the FRIPON detections in Romania resulted (Figure 1).

In Figure 2 we show the R.A. and the decl. of the radiant of the meteoroids selected for our study. This shows that the selected meteors seem to be randomly distributed in the sky. All of them are sporadic meteors.

¹² <https://www.ncei.noaa.gov/products/weather-climate-models/global-forecast>

¹³ <https://www.ecmwf.int/>

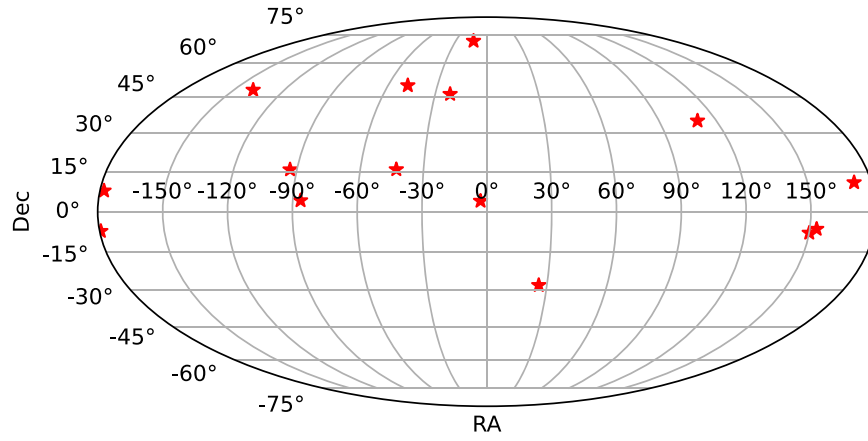


Figure 2. Sky distribution of detected meteoroids radiant.

3.2. Identification of Meteorite Producing Fireballs

As a further application of the α - β algorithm we mention the computation of the mass of the meteoroid. In Gritsevich (2008) the authors used Equation (13) in order to determine the mass of the meteoroid at the entry in the atmosphere as:

$$M_e = \left(\frac{1}{2} c_d \frac{\rho_0 h_0}{\alpha \sin \gamma} \frac{A_e}{\rho_m^{2/3}} \right)^3. \quad (16)$$

In Equation (16) $A_e = \frac{S_e}{W_e^{2/3}}$ represents the shape factor and W_e is the volume of the meteoroid.

Furthermore, the final mass of the meteoroid (the mass computed at the end of the ablation phenomenon) can be determined from Equation (11) as:

$$M_f = M_e \exp \left\{ -\frac{\beta}{1-\mu} \left[1 - \left(\frac{V_f}{V_e} \right)^2 \right] \right\}, \quad (17)$$

where V_f is the velocity of the meteoroid at the end of the luminous trajectory.

We follow the method proposed in Sansom et al. (2019) in order to compute the final mass and we consider the case when the final velocity is much smaller than the entry velocity ($\left(\frac{V_f}{V_e}\right)^2 \rightarrow 0$). Under the latter assumption, Equation (17) becomes (Sansom et al. 2019):

$$M_f = M_e \exp \left\{ -\frac{\beta}{1-\mu} \right\}. \quad (18)$$

We introduce the parameter M_e^* like in Sansom et al. (2019) as:

$$M_e^* = \left(\frac{1}{2} \frac{c_d \rho_0 h_0 A_e}{\rho_m^{2/3}} \right)^3 \quad (19)$$

so that

$$M_e = \frac{1}{\alpha^3 \sin^3 \gamma} M_e^*.$$

Thus (18) becomes (Sansom et al. 2019):

$$M_f = \frac{1}{\alpha^3 \sin^3 \gamma} M_e^* \exp \left\{ -\frac{\beta}{1-\mu} \right\}. \quad (20)$$

The mass-loss parameter β can be written as a function of ballistic coefficient α (Sansom et al. 2019):

$$\beta = (\mu - 1) \left[\ln \left(\frac{M_f}{M_e^*} \right) + 3 \ln(\alpha \sin \gamma) \right]. \quad (21)$$

Thus, the boundaries that separate the domain in three regions (“likely fall,” “possible fall,” and “unlikely fall”) are:

$$\mu = 0, \quad \ln \beta = \ln \left[-\ln \left(\frac{M_f}{M_e^*} \right) - 3 \ln(\alpha \sin \gamma) \right] \quad (22)$$

and

$$\mu = \frac{2}{3}, \quad \ln \beta = \ln \left[-\frac{1}{3} \ln \left(\frac{M_f}{M_e^*} \right) - \ln(\alpha \sin \gamma) \right]. \quad (23)$$

The entry mass M_e is computed introducing in Equation (16) the values $\rho_0 = 1.29 \text{ kg m}^{-3}$ (the density of air near the Earth’s surface) and $h_0 = 7160 \text{ m}$ (the height of the homogeneous atmosphere). Let M_1 and M_2 be the mass of meteoroids having a spherical shape and a parallelepiped shape, respectively. In order to compute the M_1 mass we take $A_e = 1.21$, $c_d = 1.0$ and $\rho_m = 3500 \text{ kg m}^{-3}$ (Gritsevich 2008). In order to determine the M_2 mass we considered the meteoroid to have a parallelepiped shape with the lengths $2L$, $3L$, and $5L$ like in Gritsevich (2008). Thus the shape factor becomes $A_e = 1.55$ (Gritsevich 2008). In Table 1 are mentioned the initial and final mass of the meteoroids (having spherical shape and parallelepiped shape, respectively) computed with Equations (16) and (17). The entry mass ranges between 0.60 and 1083.4 g (as seen in Table 1), which cumulatively counts 3610 g for $A_e = 1.21$. In the case when $A_e = 1.55$ the entry mass of the studied sample ranges from 1.3 to 2277.3 g; this leads to a total mass of 7600 g. The remnant matter after the ablation is 130 g for $A_e = 1.21$ and 270 g for $A_e = 1.55$. The total events considered for this study and the stations that detected them can be seen in the Zenodo database (10.5281/zenodo.6644650). The fireballs were recorded with the use of 13 all-sky FRIPON–MOROI cameras (see the Zenodo database 10.5281/zenodo.6626839), which were installed in Romania over the course of the year 2021. We analyzed the events captured in time period between 2021 January 7 and 2022 April 24.

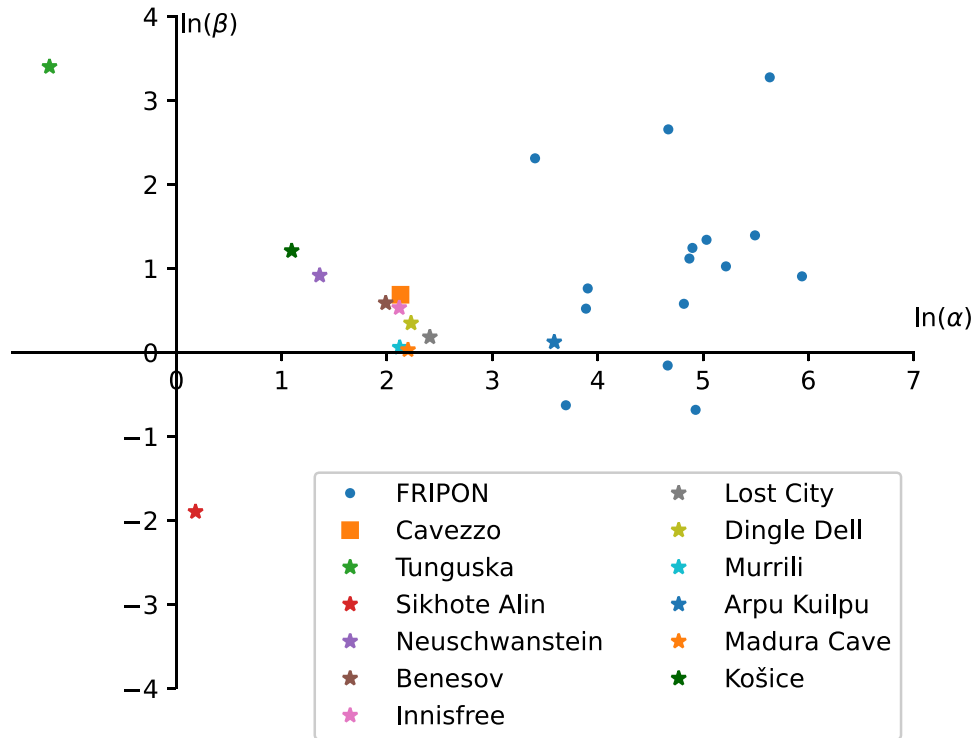


Figure 3. Distribution of the α and β parameters. Note that each event has an individual trajectory slope. The α and β parameters for the Cavezzo meteorite are computed from Gardiol et al. (2021). The α and β values for the Tunguska, Sikhote-Alin, Neuschwanstein, Benešov, Innisfree, and Lost City meteorites are mentioned in Gritsevich et al. (2012). The values for the other important detections can be found in: Devillepoix et al. (2018) (for the Dingle Dell meteorite), Sansom et al. (2020) (for the Murrili meteorite), Shober et al. (2022) (for the Arpu Kuilpu meteorite), Devillepoix et al. (2022) (for the Madura Cave meteorite), and Gritsevich et al. (2017) (for the Košice meteorite).

Table 1
Mass of Meteoroids

Event	M_1 (g)	M_1 (g)	M_2 (g)	M_2 (g)
	Entry (g)	Final (g)	Entry (g)	Final (g)
20210107T182410	11.2	0	23.5	0
20210303T035840	188.0	0.3	395.3	0.7
20210327T232051	0.6	0	1.3	0
20210525T190753	1.1	0	2.3	0
20210713T192932	36.4	4.3	76.6	9.2
20210903T193410	8.8	0	18.5	0
20210904T202357	11.1	1.0	23.4	2.3
20210910T184600	545.1	0	1146.0	0
20210926T210704	181.9	1.3	382.4	2.9
20211024T192057	219.9	48.8	462.2	102.7
20220130T155708	731.0	0	1536.6	0
20220310T223953	15.8	0.1	33.2	0.3
20220321T224005	48.5	16.5	102.0	34.7
20220325T223826	1083.4	21.3	2277.3	44.7
20220329T221413	533.3	38.4	1121.0	80.9

4. Distribution of the α and β Parameters for Selected Fireballs

In Figure 3 we made a graphical representation of the α and β parameters for the FRIPON detections in $(\ln \alpha, \ln \beta)$ coordinates. We plot the FRIPON events detected by the MOROI stations in Romania, together with the meteorite Cavezzo, and some events already present in literature. The Cavezzo meteorite (Gardiol et al. 2021) is the meteorite recovered by the PRISMA component of FRIPON in Italy. Other representations of meteoroids in the $(\ln \alpha, \ln \beta)$ plane can be found in the literature

(Gritsevich et al. 2012; Sansom et al. 2019; Moreno-Ibáñez et al. 2020). The meteoroids that result in a meteorite production can be found in a cluster region (Figure 3: Košice, Tunguska, Neuschwanstein, Benešov, Innisfree, Lost City, Dingle Dell, Murrili, Arpu Kuilpu, Madura Cave).

In Figures (4)–(6) we present the outcome for the FRIPON detections. We have one event (20211024T192057) that could produce meteorites of the ground. The all-sky images of the detection can be found in Figure 7. This result is good taking into account the time period of a year and the fact that in France during the timespan of a year a meteorite with the final mass of 500 g and three objects with masses smaller than 100 g are reported (Colas et al. 2020) with the use of 106 cameras.

If we want to compute the meteoroid’s final mass, the parameters that we take into account in our study are the dimensionless shape factor at the entry in the atmosphere A_e and the bulk density ρ_m . Depending on the choice of the input values of these parameters we obtain different results for the objects selected for our study.

In order to identify fireballs that produce meteorites we follow the procedure described in Sansom et al. (2019) and we make some simulations on the meteoroid shape factor at entry A_e , bulk density ρ_m , and final mass M_f . In order to mathematically define the production of meteorites we need to set up a minimum required mass that would imply the feasibility of recovering a meteorite with a mass smaller than a set value. This is needed in order to depict the real world as mathematical work. In cases 1–3 below we impose the set values of 50 g and 25 g for the final mass. Meteorites with small final masses are visible when the terrain is good. In 2019 a search campaign was carried out in Australia when the meteorite Arpu Kuilpu with the final mass of

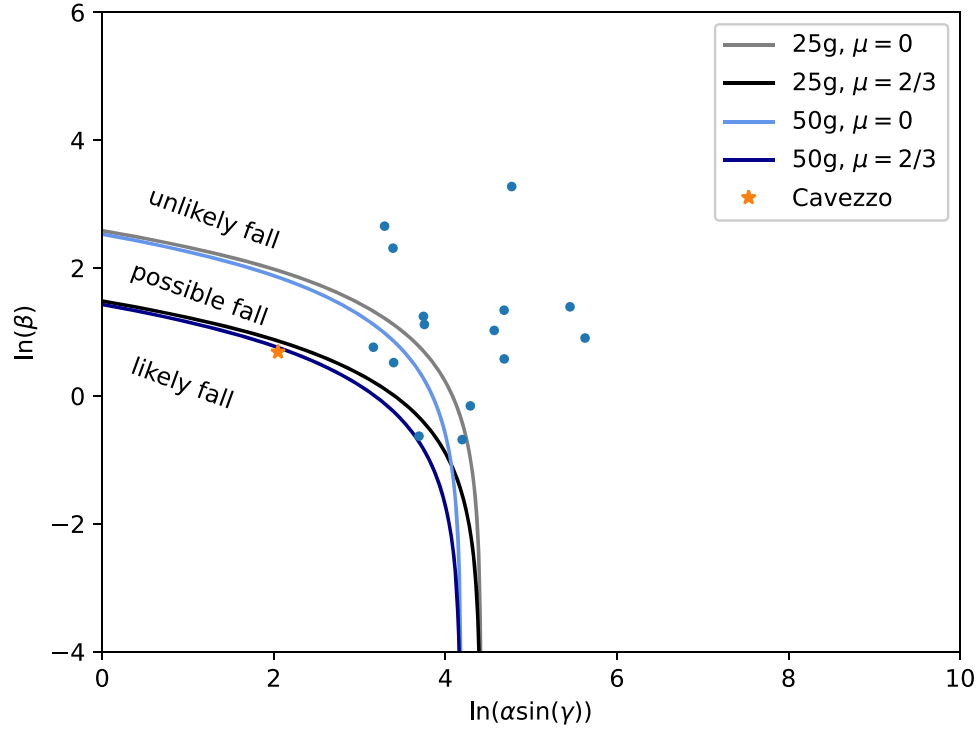


Figure 4. Outcome for selected FRIPON detections. The boundaries for different minimum terminal mass assumptions are shown. The input parameters are: $c_d = 1$, $A_e = 1.21$, $\rho_m = 3500 \text{ kg m}^{-3}$.

42 g was recovered (Shober et al. 2022) by The Desert Fireball Network. This is the first time when a search campaign was carried out in order to recover an object with such a small mass.

Case 1—Outcome for meteoroids with a spherical shape. The cases $M_f = 50 \text{ g}$ and $M_f = 25 \text{ g}$ are considered.

We consider the case $M_f = 50 \text{ g}$, $c_d = 1.0$, $\rho_m = 3500 \text{ kg m}^{-3}$, $A_e = 1.21$, and we obtain $\ln(M_f/M_e^*) = -12.55$ and the boundaries:

$$\mu = 0, \ln \beta = \ln \{12.55 - 3 \ln(\alpha \sin \gamma)\}, \quad (24)$$

$$\mu = \frac{2}{3}, \ln \beta = \ln \{4.18 - \ln(\alpha \sin \gamma)\}. \quad (25)$$

In order to find the outcome for meteoroids having the final mass 25 g we make the following simulation. We consider $M_f = 25 \text{ g}$, $c_d = 1.0$, $\rho_m = 3500 \text{ kg m}^{-3}$, $A_e = 1.21$.

We obtained $\ln(M_f/M_e^*) = -13.25$ and the boundaries:

$$\mu = 0, \ln \beta = \ln \{13.25 - 3 \ln(\alpha \sin \gamma)\}, \quad (26)$$

$$\mu = \frac{2}{3}, \ln \beta = \ln \{4.41 - \ln(\alpha \sin \gamma)\}. \quad (27)$$

The boundaries given by Equations (24)–(27) and the points of coordinates $(\ln(\alpha \sin \gamma), \ln \beta)$ corresponding to each meteoroid are represented in Figure 4.

Case 2—Outcome for meteoroids with a shape factor $A_e = 1.55$. The cases $M_f = 50 \text{ g}$ and $M_f = 25 \text{ g}$ are considered.

To account for the case of a meteoroid with a shape factor $A_e = 1.55$ (as an example we mention meteoroids with parallelepiped shape) we rewrite the cases above as follows: if $M_f = 50 \text{ g}$, $c_d = 1.0$, $\rho_m = 3500$, and $A_e = 1.55$ then $\ln(M_f/M_e^*) = -13.30$. Thus the boundaries are:

$$\mu = 0, \ln \beta = \ln \{13.30 - 3 \ln(\alpha \sin \gamma)\}, \quad (28)$$

$$\mu = \frac{2}{3}, \ln \beta = \ln \{4.43 - \ln(\alpha \sin \gamma)\}. \quad (29)$$

In the assumption of $M_f = 25 \text{ g}$, $c_d = 1.0$ and $A_e = 1.55$ then $\ln(M_f/M_e^*) = -13.99$. We obtain the boundaries:

$$\mu = 0, \ln \beta = \ln \{13.99 - 3 \ln(\alpha \sin \gamma)\}, \quad (30)$$

$$\mu = \frac{2}{3}, \ln \beta = \ln \{4.66 - \ln(\alpha \sin \gamma)\}. \quad (31)$$

The boundaries given by Equations (28)–(31) and the points of coordinates $(\ln(\alpha \sin \gamma), \ln \beta)$ corresponding to each meteoroid are represented in Figure 5.

Case 3—Outcome for meteoroids with a spherical shape. The density values $\rho_m = 2700 \text{ kg m}^{-3}$ and $\rho_m = 3500 \text{ kg m}^{-3}$ are considered.

If $M_f = 50 \text{ g}$, $c_d = 1.0$, $A_e = 1.21$, and $\rho_m = 2700 \text{ kg m}^{-3}$ then $\ln(M_f/M_e^*) = -13.07$. The boundaries become:

$$\mu = 0, \ln \beta = \ln \{13.07 - 3 \ln(\alpha \sin \gamma)\}, \quad (32)$$

$$\mu = \frac{2}{3}, \ln \beta = \ln \{4.35 - \ln(\alpha \sin \gamma)\}. \quad (33)$$

The boundaries given by Equations (24)–(25) (for $\rho_m = 3500 \text{ kg m}^{-3}$) and (32)–(33) (for $\rho_m = 2700 \text{ kg m}^{-3}$), and the points of coordinates $(\ln(\alpha \sin \gamma), \ln \beta)$ corresponding to each meteoroid are represented in Figure 6.

The shape coefficient μ is related to the rotation of the meteoroid. If $\mu = 0$ then the meteoroid does not spin and if $\mu = \frac{2}{3}$ then the meteoroid spins uniformly (Sansom et al. 2019). If $\mu = 0$ then the ablation phenomenon occurs only on the front side of the object, while if $\mu = \frac{2}{3}$ then the meteoroid ablates uniformly.

Case 4—Arbitrary case.

To estimate the outcome that is different from those three cases that we exemplified above, one can simply recalculate the mass values as in Gritsevich (2009). If the values of A_e , c_d , and ρ_m are different than the ones mentioned earlier in this work,

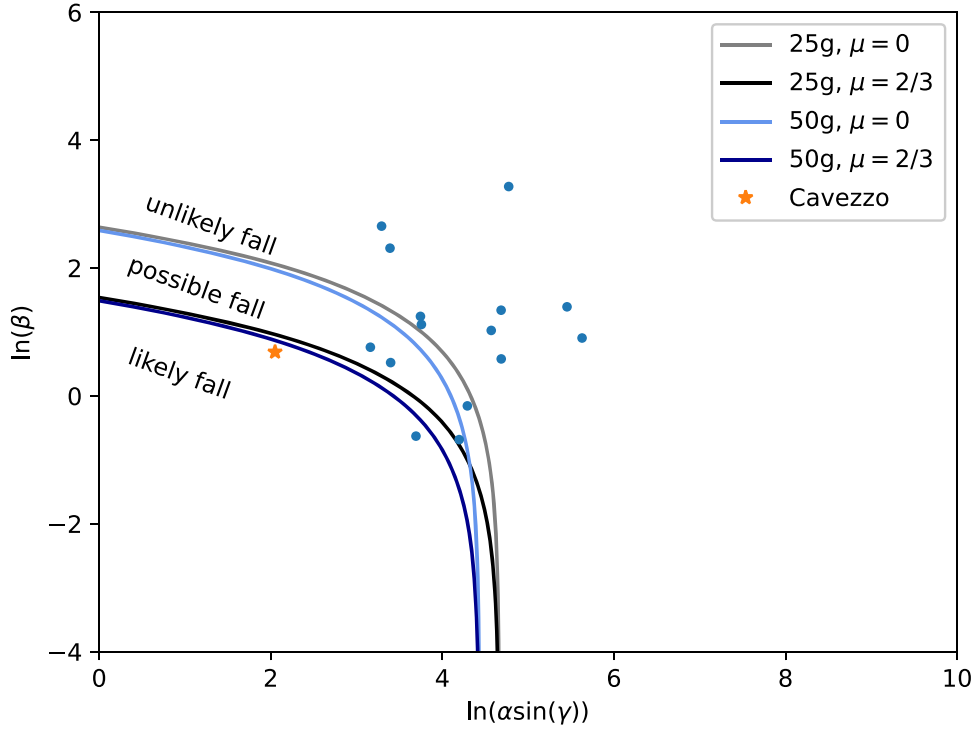


Figure 5. Outcome for selected FRIPON detections. The boundaries for different minimum terminal mass assumptions are shown. The input parameters are: $c_d = 1$, $A_e = 1.55$, $\rho_m = 3500 \text{ kg m}^{-3}$. Determination of α and β does not require any other parameters to be a priori assumed. Assumptions are made only for the curves.

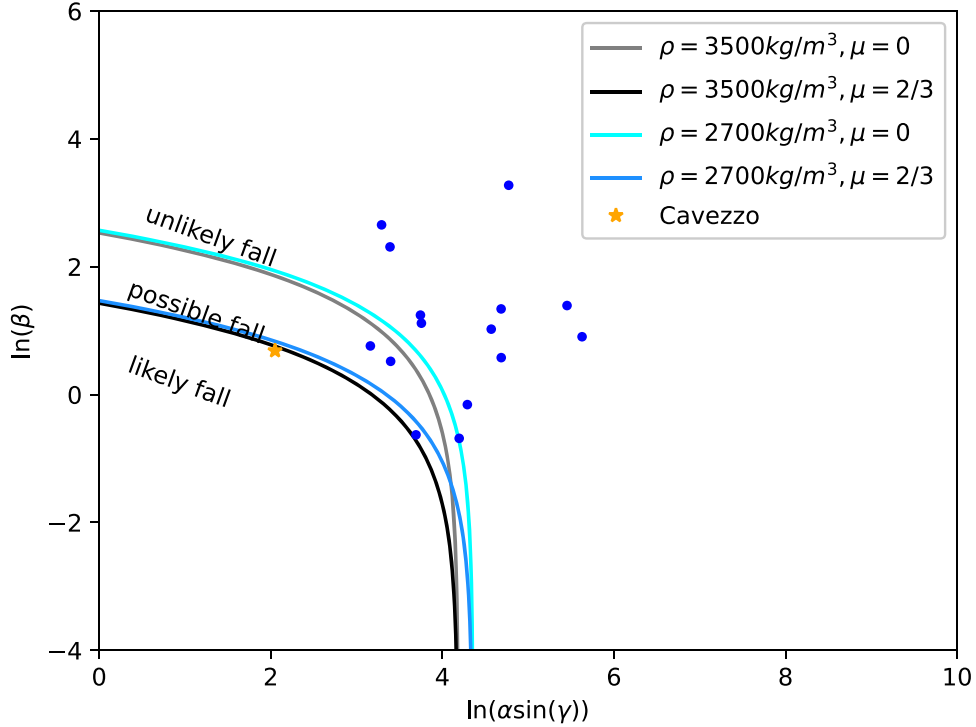


Figure 6. Outcome for selected FRIPON detections. The boundaries for different minimum terminal mass assumptions are shown. The input parameters are $c_d = 1$, $A_e = 1.21$, $m = 50 \text{ g}$.

then the entry mass can be computed as (Gritsevich 2009):

$$\frac{M_{e1}}{M_{e2}} = \left(\frac{c_{d1} A_{e1}}{c_{d2} A_{e2}} \right)^3 \left(\frac{\rho_{m2}}{\rho_{m1}} \right)^2, \quad (34)$$

where $(c_{d1}, A_{e1}, \rho_{m1})$, $(c_{d2}, A_{e2}, \rho_{m2})$ are two value sets of the input parameters. From (19) we obtain $\frac{M_{e1}^*}{M_{e2}^*} = \frac{M_{e1}}{M_{e2}}$. If we compute M_{e1}^* then M_{e2}^* is easily obtained from (34).

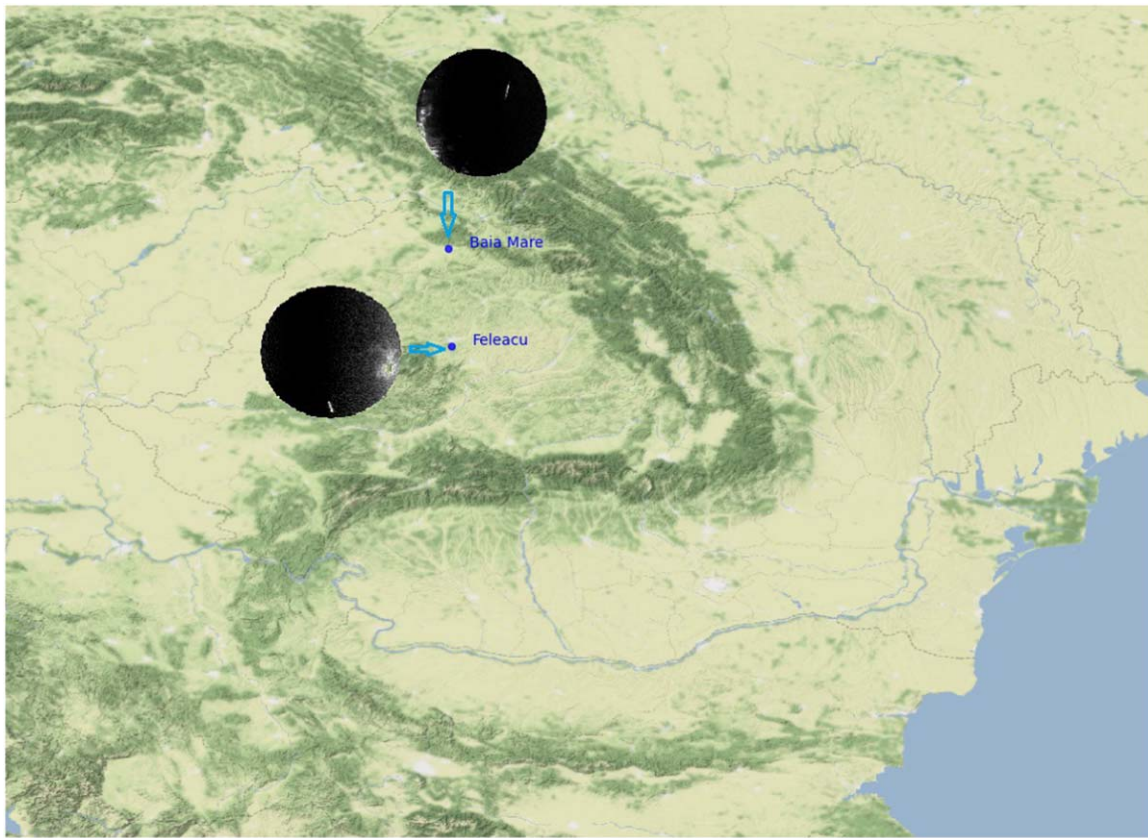


Figure 7. Meteoroid detected 20211024T192057 by stations Feleacu (ROCJ01) and Baia Mare (ROMM01).

4.1. Meteorite Candidate—The Meteoroid Detected at 20211024T192057

Hereinafter we present the luminous trajectory of a meteoroid detected at 20211024T192057 that, as further seen in Section 4, is likely to produce a meteorite on the ground.

Figure 8 shows the velocity during the luminous trajectory as an approximation on groups of five points for the meteoroid detected by stations Baia Mare (ROMM01) and Feleacu (ROCJ01) at 2021 October 24, 19:20:57 UT. In Figure 9 is represented the height of the meteoroid during the luminous trajectory.

The input values for determining α and β are the meteoroid slope, height, and velocity. The height and velocity of the meteoroid from the FRIPON database were determined as explained in Jeanne et al. (2019) and Colas et al. (2020). In order to work with dimensionless velocity and height, the velocity is normalized to the initial velocity (in this article considered to be the mean of the first 10 velocities measured during the luminous trajectory), while the height is normalized to the height of the homogeneous atmosphere.

In Table 2 are presented the meteoroid velocity and height at the end of the luminous trajectory, the computed slope and the values of α and β computed with the algorithm described in the previous section.

In Figure 10 we plot the dimensionless height and velocity for the meteoroid that can likely produce meteorites, as further seen in this work.

In order to explore the past dynamical evolution of 20211024T192057 bolide’s parent body, we performed a backward numerical integration of 1500 clones for the last 100,000 yr. The clones were randomly generated using a

Gaussian distribution of the six orbital elements using the nominal and the 1σ values found by the meteor trajectory computation procedure. Despite the chaotic behavior (Figure 11), typical for the inner region of the solar system, only three clones were lost during the integration during a close approach with the Sun. For 11% of the clones (172) we recorded extreme close approaches (<10 Roche limits) with Venus (91%), Earth (5%), and Mercury (4%). Clones’ evolution is mostly confined in a region dominated by two powerful resonances 4:1 J (2.064 au) and 1:3 E (2.080 au; Vakhidov 1999; Gallardo 2006) indicating that the precursor body of the detected bolide might be a relatively long time resident of the inner solar system.

4.2. Discussion

This paper presents a classification of the fireball detections observed by the FRIPON–MOROI Network from the beginning of 2021 until 2022 April 24. The FRIPON–MOROI Network detected over 100 meteors, 13.88% satisfying the criterion of noticeable deceleration ($V_f/V_0 < 0.8$). The luminous trajectory of the sample of meteoroids analyzed in this work can be found in Figure 12.

We processed the whole database of FRIPON detections in Romania in order to distinguish the ones suitable for dark flight. The detection of FRIPON images is made with the FreeTure software. If two or more meteors are detected within a time period less than 3 s by cameras having the distance between them less than 190 km, then the detection is classified as a “multiple detection.” This process is described in detail in Colas et al. (2020).

The main steps of the algorithm used in this paper are:

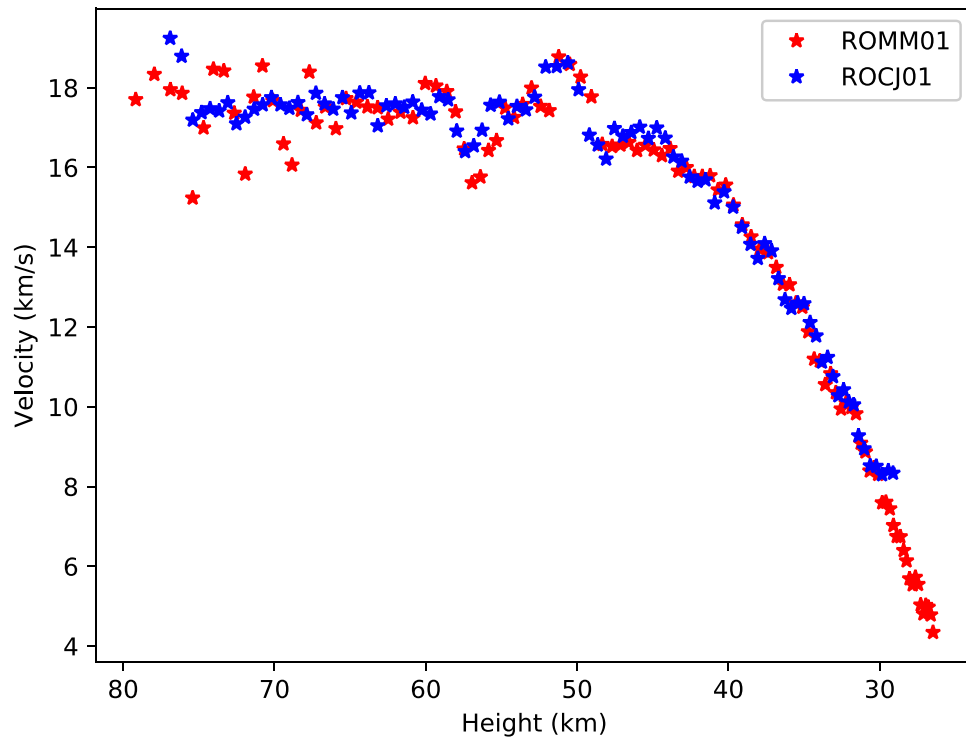


Figure 8. The velocity during luminous phenomenon computed by FRIPON using a linear approximation on groups of five points for the fireball detected at 20211024T192057.

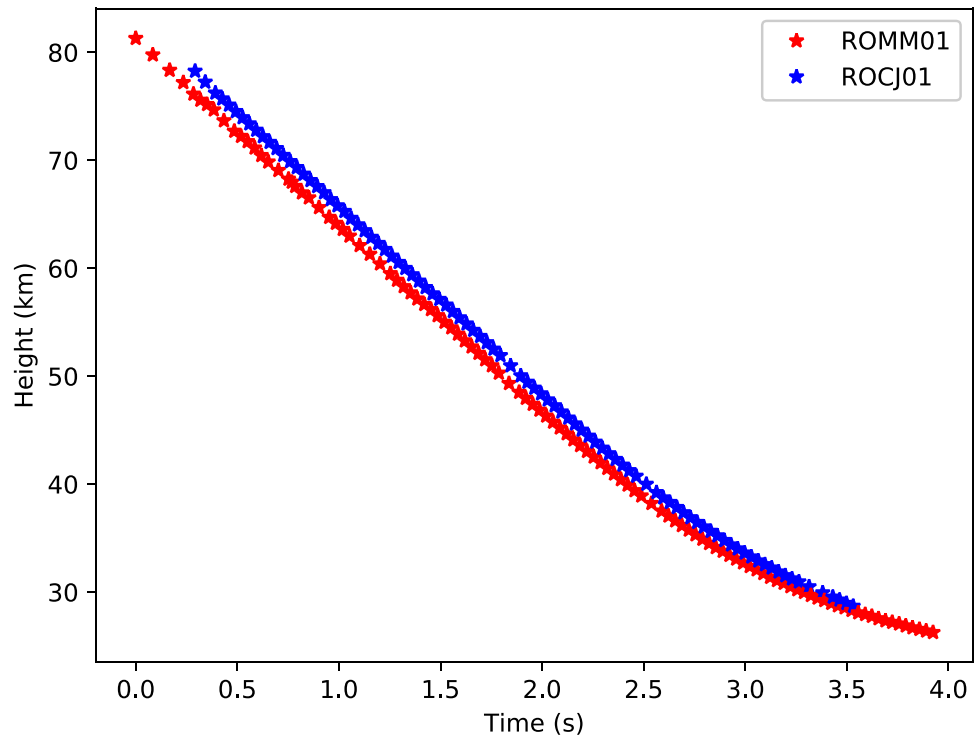


Figure 9. The altitude during luminous phenomenon of the event detected at 20211024T192057.

1. Compute the velocity of the meteoroid during the luminous trajectory;
2. Compute the slope γ of the trajectory;
3. Determine the initial velocity of the meteoroid;
4. Normalize the velocity of the meteoroid to initial velocity, normalize the height of the meteoroid to the height of the homogeneous atmosphere (7160 m), and obtain Equations (9) and (10);

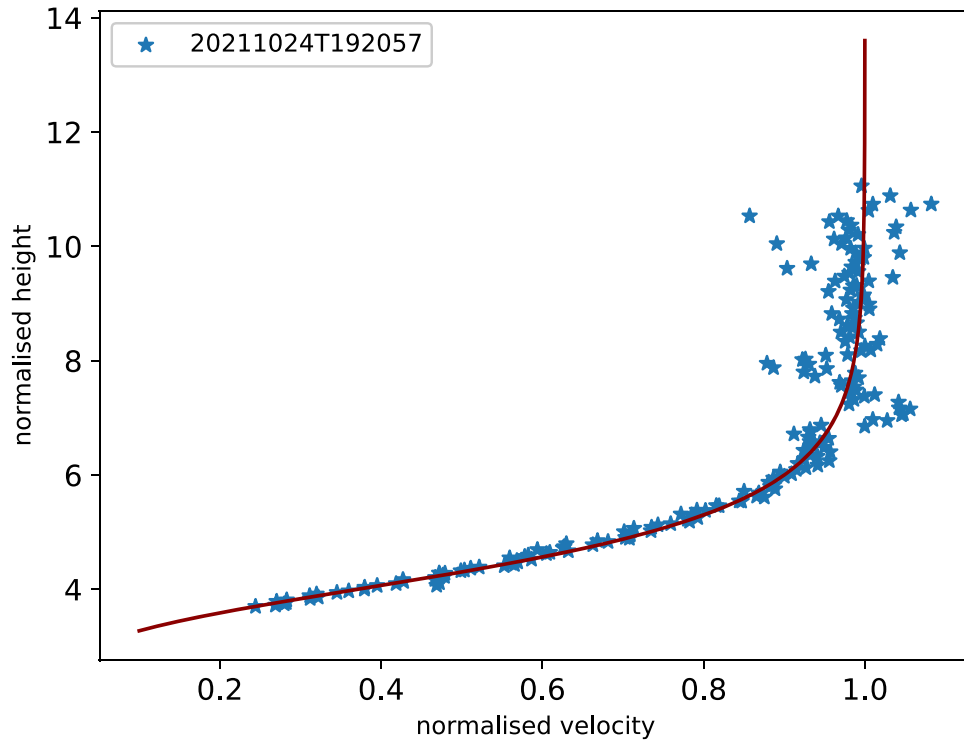


Figure 10. Normalized velocity (V/V_0) and height for the meteor detected at 20211024T192057.

Table 2

Detections with Deceleration Obtained by FRIPON over Romania During the Time Period 2021–2022

Event	V_{end} (km/s)	H_{end} (km)	γ ($^\circ$)	α	β
20210107T182410	15.664	48.737	44.89	153.46	3.82
20210303T035840	17.845	47.106	18.37	134.22	3.46
20210327T232051	16.683	56.421	47.10	379.83	2.47
20210525T190753	13.308	53.240	73.83	243.14	4.02
20210713T192932	8.344	37.627	43.52	106.14	0.85
20210903T193410	26.282	64.981	25.02	277.33	26.72
20210904T202357	11.684	45.780	61.18	123.79	1.78
20210910T184600	16.627	42.052	79.97	30.13	10.08
20210926T210704	9.184	47.076	19.14	130.42	3.05
20211024T192057	4.342	26.481	84.11	40.37	0.53
20220130T155708	12.223	53.880	14.58	106.83	14.21
20220310T223953	13.207	48.977	31.54	184.54	2.78
20220321T224005	9.343	40.251	28.70	138.36	0.50
20220325T223826	9.712	36.818	28.35	49.68	2.14
20220329T221413	15.237	38.563	37.71	48.86	1.68

5. Compute α and β that minimize the expression in (15);
6. Find the solution (11)–(12) of Equations (9) and (10);
7. Plot the curves corresponding to the minimum and maximum of the dimensionless parameter μ ($\mu = 0$ and $\mu = 2/3$, respectively) that separate the domain in three regions: “likely fall,” “possible fall,” and “unlikely fall.”

Figures (4)–(6) show the different case scenarios (the meteorite Cavezzo lies in the “likely fall” region in all cases). Meteoroid 20211024T192057 [3.69, -0.62] is another candidate that lies in the “likely fall” region in the case when the final mass is less than 25 g (whether it has a spherical or parallelepiped shape; Figures 4 and 5). If we consider the final mass less than 50 g, then the object lies in the “likely fall”

region for $\rho = 2700 \text{ kg m}^{-3}$ and spherical shape (Figure 6) or for $\rho = 3500 \text{ kg m}^{-3}$ and spherical shape (Figure 5). If the final mass is less than 50 g and $\rho = 3500 \text{ kg m}^{-3}$ and considering spherical shape then the meteoroid lies in the “possible fall” region (Figure 4). Meteoroid 20220321T224005 [4.19, -0.68] lies in the “possible fall” region whether it has a spherical shape and final mass less than 25 g (Figure 4), or a parallelepiped shape (Figure 5). If it has a spherical shape and the density $\rho = 3500 \text{ kg m}^{-3}$ then it is unlikely to fall on the ground (Figures 4 and 6). Meteoroids 20220325T223826 [3.16, 0.76] and 20220329T221413 [3.39, 0.52] lie in the “possible fall” regions in all case scenarios (Figures 4–6). Meteoroid 20210713T192932 [4.29, -0.15] has the outcome of a “possible fall” only in the case of a parallelepiped shape, final mass less than 25 g, and $\rho = 3500 \text{ kg m}^{-3}$ (Figure 5).

Considering the events in the “likely fall” and “possible fall” regions, the remaining mass after the ablation phenomenon is 120 g for $c_d = 1.0$, $A_e = 1.21$, and $\rho = 3500 \text{ kg/m}^3$. In the case $c_d = 1.0$, $A_e = 1.55$, and $\rho = 3500 \text{ kg m}^{-3}$, the final mass of the meteoroids that reach the ground is 260 g.

Based on the values of the entry mass and final mass computed for the sample of events with deceleration, we want to compute the total mass for the meteoroids with noticeable deceleration entering the atmosphere of the Earth. We estimate that the MOROI cameras capture all-sky images within an area of 393,853 km². Thus, we obtain that the total entry mass for meteoroids with noticeable deceleration entering the atmosphere of the Earth during the studied time period is 4685.28 kg for $A_e = 1.21$ and 9848.60 kg for $A_e = 1.55$. The remnant matter after the ablation phenomenon is 171.81 kg for $A_e = 1.21$ and 361.15 kg for $A_e = 1.55$.

In Gritsevich (2009) the parameters α and β are computed for the Prairie Network fireballs and Canadian Network fireballs with decelerations. Parameters α and β have been

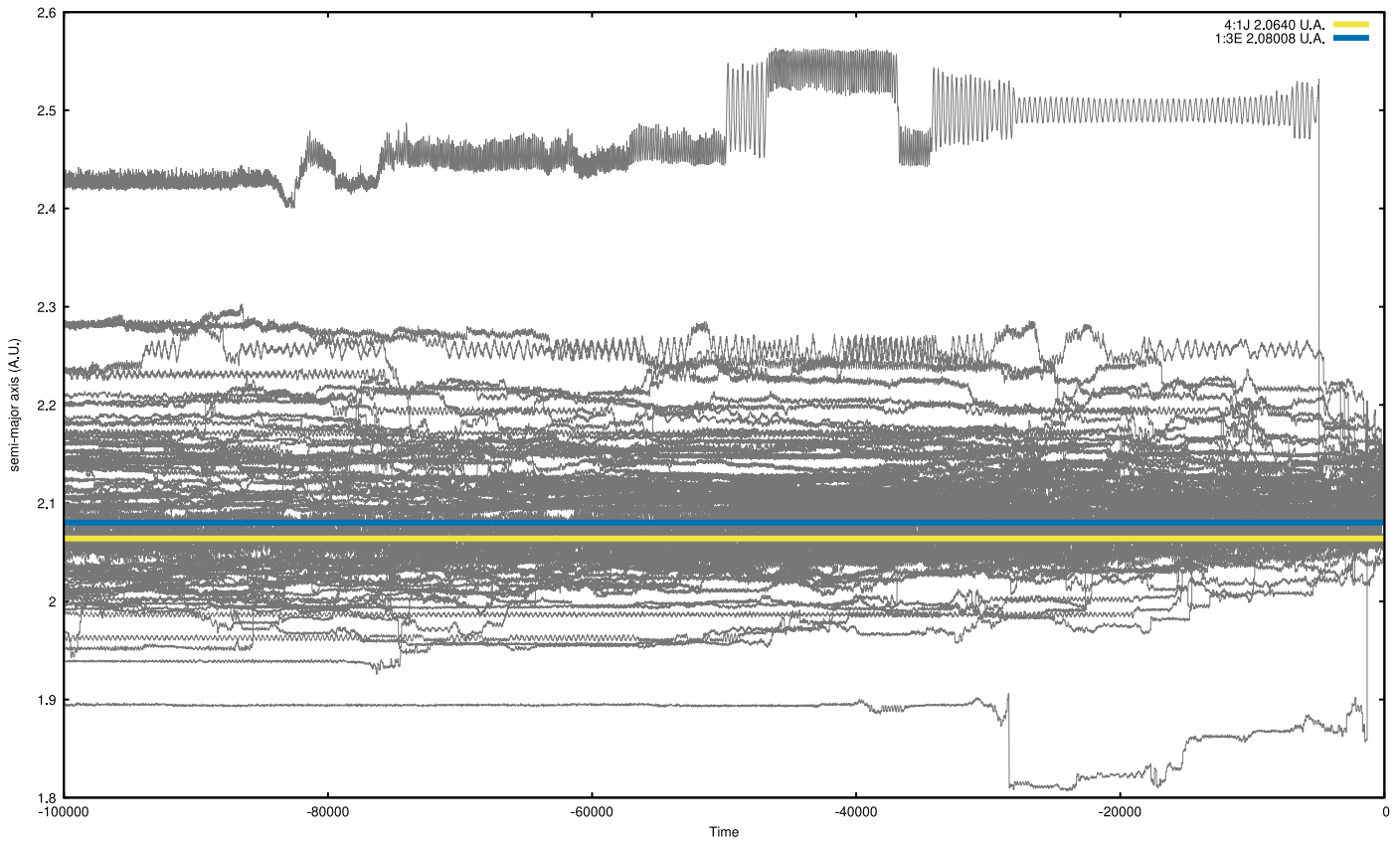


Figure 11. Semimajor axis evolution for the last 100,000 yr for a representative set of clones of 20211024T192057 bolide.

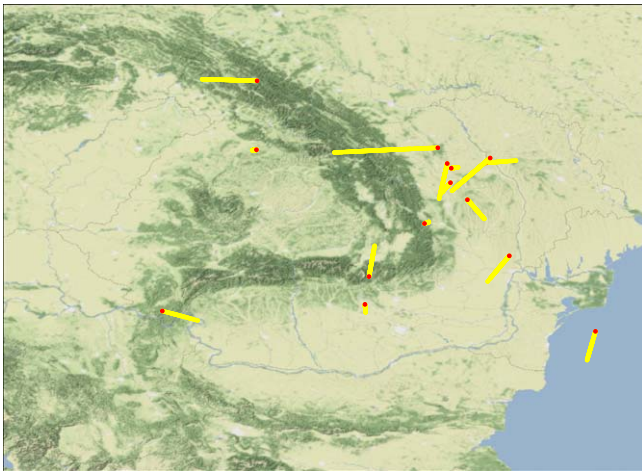


Figure 12. Projection of luminous trajectories on map. The final point of the luminous trajectory is marked with red.

determined for detections of the Canadian Network, for the US Prairie Network, and for Benešov bolide in Gritsevich (2007).

On a larger scale of time the MOROI Network is expected to record more fireball events that have outcomes as those mentioned below. In Gritsevich et al. (2012) is presented a way of using the α - β algorithm in order to determine the outcome of a collision of an object with the atmosphere and with the surface of the Earth. In the case when $\alpha \ll 1$, $\beta \ll 1$ the collision with Earth would result in a massive crater (e.g., the Barringer crater in Arizona). If $\alpha \sim 1$, $\beta < 1$ then the body would be destroyed in the atmosphere and the resulting

fragments would produce craters on Earth (e.g., Sikhote-Alin). If $\alpha \sim 1$, $\beta \sim 1$ then ablation plays a higher role and smaller fragments would reach the Earth without producing craters (e.g., Neuschwanstein, Innisfree, Lost City). If $\alpha < 1$, $\beta \gg 1$ then the meteoroid would be destroyed and fully destroyed in the atmosphere (e.g., Tunguska; Gritsevich et al. 2012).

In Sansom et al. (2019) the authors use the method presented in Gritsevich (2008) in order to classify the 278 detections of the Desert Fireball Network with noticeable deceleration ($V_f/V_0 < 0.8$) into three categories: meteoroids that are likely to result in meteorites on the ground, meteoroids that can possibly be meteorite droppers, and meteoroids that are unlikely to produce meteorites.

5. Conclusions and Future Work






In this paper we used the α - β algorithm in order to study the meteors detected by the FRIPON in Romania. We analyze only the events with noticeable deceleration. We determine the parameters α and β for the selected sample. We classified the events in three categories: (1) meteoroids likely to produce meteorites; (2) meteoroids that can possibly produce meteorites; (3) meteoroids unlikely to produce meteorites. The entry and final mass are determined for each event. We identified a meteoroid likely to produce a meteorite on the ground (the meteoroid detected at 20211024T192057). We explored the past dynamical evolution of the parent body of this meteoroid.

The main importance of this work is that it allows us to quickly select the fireball events that require a follow-up. We are the first to compute the α and β parameters for the Cavezzo meteorite; the fact that it lies in the “likely fall” region validates our results. We obtained great results after the installation of

the FRIPON cameras in Romania and taking into account that the cameras were installed during the time of 1 year. The results obtained here are a good means of showing what results can be achieved by the FRIPON network installed in a new country in 16 months of functionality. This is very useful material for countries that want to initiate new collaborations with FRIPON. This algorithm will be further applied to future detections of FRIPON. The total entry mass of the studied events is 3610 g if the meteoroids have a spherical shape and 7600 g if the objects have a parallelepiped shape. The total remnant matter after the ablation is 130 g if the detected objects have spherical shape and 270 g in the case of a parallelepiped shape. In a future study we will apply the α - β algorithm to events without deceleration. Furthermore we aim at introducing into the code a build-in recalculation for the realistic atmospheric conditions after Lyytinen & Gritsevich (2016) and see how these could improve the results. We will also calculate the dark-flight trajectory for events identified in the “likely fall” and “possible fall” regions with the algorithms presented in Vinnikov et al. (2016), Moilanen et al. (2021), and Boaca et al. (2021). We plan to apply the algorithm to detections of the FRIPON in other countries.

The work of I.B. and M.B. was supported by a grant of the Ministry of Research, Innovation and Digitization, CNCS-UEFISCDI, project No. PN-III-P1-1.1-PD-2019-0784, within PNCDI III. M.G. acknowledges the Academy of Finland project No. 325806 (PlanetS). The work of A.N. was supported by a grant of the Ministry of National Education and Scientific Research, PNIII-P2-1214/25.10.2021, program No. 36SOL/2021.

ORCID iDs

Ioana Boaca  <https://orcid.org/0000-0001-7481-0362>
 Maria Gritsevich  <https://orcid.org/0000-0003-4268-6277>
 Mirel Birlan  <https://orcid.org/0000-0003-3495-8535>
 Tudor Boaca  <https://orcid.org/0000-0002-4839-8949>
 Pierre Vernazza  <https://orcid.org/0000-0002-2564-6743>

References

- Abramowitz, M., & Stegun, I. A. 1964, Handbook of Mathematical Functions with Formulas, Graphs, and Mathematical Tables (Washington, DC: U. S. Dept. of Commerce, National Bureau of Standards)
- AIAA G-003C-2010 2010, Guide to Reference and Standard Atmosphere Models (Reston, VA: AIAA)
- Barucci, M. A., Yoshikawa, M., Michel, P., et al. 2009, *ExA*, **23**, 785
- Boaca, I., Nedelcu, A., Birlan, M., Boaca, T., & Anghel, S. 2021, *RoAJ*, **31**, 171
- Colas, F., Zanda, B., Bouley, S., et al. 2020, *A&A*, **644**, A53
- Devillepoix, H. A. R., Sansom, E. K., Bland, P. A., et al. 2018, *MAPS*, **53**, 2212
- Devillepoix, H. A. R., Sansom, E. K., Shober, P., et al. 2022, *M&PS*, **57**, 1328
- Droshagen, E., Ott, T., Koschny, D., et al. 2021, *A&A*, **650**, A159
- Gallardo, T. 2006, *Icar*, **184**, 29
- Gardioli, D., Barghini, D., Buzzoni, A., et al. 2021, *MNRAS*, **501**, 1215
- Grady, M. M., & Wright, I. 2006, in Meteorites and the Early Solar System II, ed. D. S. Lauretta & H. Y. McSween (Tucson, AZ: Univ. Arizona Press), **3**
- Gritsevich, M., Dmitriev, V., Vinnikov, V., et al. 2017, in Assessment and Mitigation of Asteroid Impact Hazards: Proc. of the 2015 Barcelona 413 Asteroid Day, ed. M. Gritsevich & H. Palme, Vol. 46 (Berlin: Springer), **153**
- Gritsevich, M., & Koschny, D. 2011, *Icar*, **212**, 877
- Gritsevich, M. I. 2007, *SoSyR*, **41**, 509
- Gritsevich, M. I. 2008, *DokPh*, **53**, 97
- Gritsevich, M. I. 2009, *AdSpR*, **44**, 323
- Gritsevich, M. I., Stulov, V. P., & Turchak, L. I. 2012, *CosRe*, **50**, 56
- Jeanne, S., Colas, F., Zanda, B., et al. 2019, *A&A*, **627**, A78
- Lyytinen, E., & Gritsevich, M. 2016, *P&SS*, **120**, 35
- Moilanen, J., Gritsevich, M., & Lyytinen, E. 2021, *MNRAS*, **503**, 3337
- Moreno-Ibáñez, M., Gritsevich, M., Trigo-Rodríguez, J. M., & Silber, E. A. 2020, *MNRAS*, **494**, 316
- Nedelcu, D. A., Birlan, M., Turcu, V., et al. 2018, *RoAJ*, **28**, 57
- Peña-Asensio, E., Trigo-Rodríguez, J. M., Gritsevich, M., et al. 2021b, *EPSC*, **EPSC2021-738**, 738
- Peña-Asensio, E., Trigo-Rodríguez, J. M., Gritsevich, M., & Rimola, A. 2021a, *MNRAS*, **504**, 4829
- Sansom, E. K., Bland, P. A., Towner, M. C., et al. 2020, *MAPS*, **55**, 2157
- Sansom, E. K., Gritsevich, M., Devillepoix, H. A. R., et al. 2019, *ApJ*, **885**, 115
- Schmitt, R. A., Wakita, H., & Rey, P. 1970, *Sci*, **167**, 512
- Shober, P. M., Devillepoix, H. A. R., Sansom, E. K., et al. 2022, *M&PS*, **57**, 1146
- Vakhidov, A. A. 1999, *BaltA*, **8**, 425
- Vinnikov, V. V., Gritsevich, M. I., & Turchak, L. I. 2016, *AIP Conf. Proc.*, **1773**, 110016
- Yoshikawa, M., Kawaguchi, J., Fujiwara, A., & Tsuchiyama, A. 2015, Hayabusa Sample Return Mission, in Asteroids IV, ed. P. Michel, F. E. DeMeo, & W. F. Bottke (Tucson, AZ: Univ. Arizona Press), **397**